Two-dimensional biosensor arrays based on surface plasmon resonance phase imaging

C. L. Wong, H. P. Ho, T. T. Yu, Y. K. Suen, Winnie W. Y. Chow, S. Y. Wu, W. C. Law, W. Yuan, W. J. Li, S. K. Kong, and Chinlon Lin

We present a biosensor design based on capturing the two-dimenstional (2D) phase image of surface plasmon resonance (SPR). This 2D SPR imaging technique may enable parallel label-free detection of multiple analytes and is compatible with the microarray chip platform. This system uses our previously reported differential phase measurement approach, in which 2D phase maps obtained from the signal (P) and reference (S) polarizations are compared pixel by pixel. This technique greatly improves detection resolution as the subtraction step can eliminate measurement fluctuations caused by external disturbances as they essentially appear in both channels. Unlike conventional angular SPR systems, in which illumination from a range of angles must be used, phase measurement requires illumination from only one angle, thus making it well suited for 2D measurement. Also, phase-stepping introduced from a moving mirror provides the necessary modulation for accurate detection of the phase. In light of the rapidly increasing need for fast real-time detection, quantification, and identification of a range of proteins for various biomedical applications, our 2D SPR phase imaging technique should hold a promising future in the medical device market.

OCIS codes: 240.6680, 170.0110.

1. Introduction

The detection of biomolecular species such as proteins is of vital importance because such information might help resolving many health-related issues. Proteins are the work houses of the cell and have important functions in both healthy and diseased states. The protein families are extremely diverse and have many differences in their physical sizes, chemical properties, and affinity constants. As a result, it becomes a challenge to accurately characterize the protein interactions.[1] On the other hand, there has been rapid development of microarrays for high throughput monitoring of DNA interactions. Significant success has been achieved in gene expression and genotyping research.[2] More recently increasing interest is drawn for protein microarrays. Potential needs are found in the areas of protein therapeutics, clinical diagnostics, and national security. For example, in the field of protein therapeutics, the use of antibody-based therapeutics in drug discovery is growing fast[1] and antibodies account for 20% of the marketed biological products.[1,3] The demand for devices capable of performing rapid screening of these affinity molecules is huge. There is therefore an urgent need to develop microarrays and the relevant sensing technologies for performing rapid diagnostic detection of a large number of proteins.

Until now, optical signal transduction techniques such as fluorescence[4] and surface plasmon resonance[5,6] (SPR) are playing major roles in protein detection. Labeling is required for fluorescence-based biosensors. It is well known that fluorescent protein molecules are quite expensive, time consuming, lack quantitative information, and suffer from bleaching after repeated reading. This makes other label-free techniques such as quartz crystal microbalance (QCM) or SPR more attractive. Among these, the physical limitations of QCM make them an unlikely candidate for microarray devices. On the other hand, SPR has been shown to be possible for imaging and arrayed applications.[7–9] SPR imaging has been

C. L. Wong, H. P. Ho (hpho@ee.cuhk.edu.hk), T. T. Yu, S. Y. Wu, W. C. Law, W. Yuan, and C. Lin are with the Center for Advanced Research in Photonics, The Chinese University of Hong Kong, China. Y. K. Suen and S. K. Kong are with the Department of Biochemistry, the Chinese University of Hong Kong, Hong Kong, China. W. Y. Chow and W. J. Li are with the Centre for Micro and Nano Systems, The Chinese University of Hong Kong, Hong Kong China.

Received 6 September 2006; revised 30 November 2006; accepted 1 December 2006; posted 5 December 2006 (Doc. ID 74719); published 3 April 2007.

0003-6935/07/122325-08$15.00/0

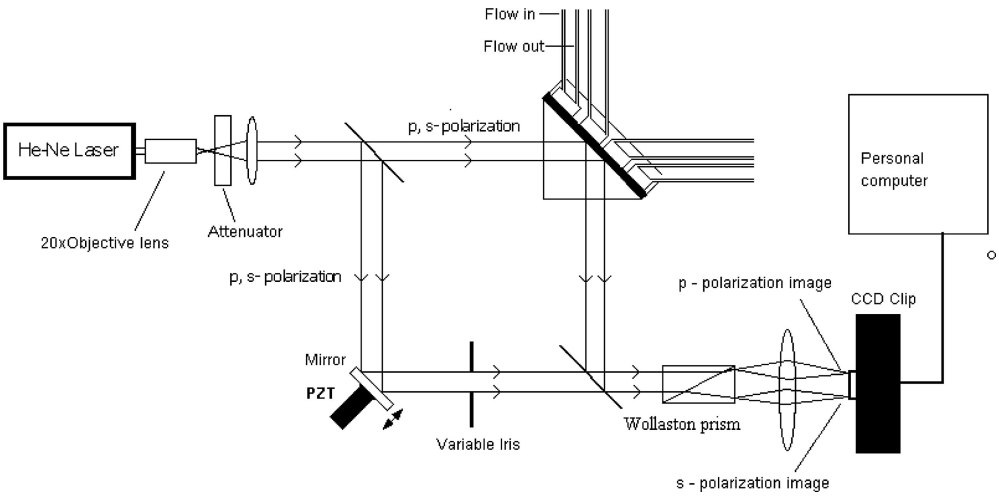

Fig. 1. Experimental scheme.

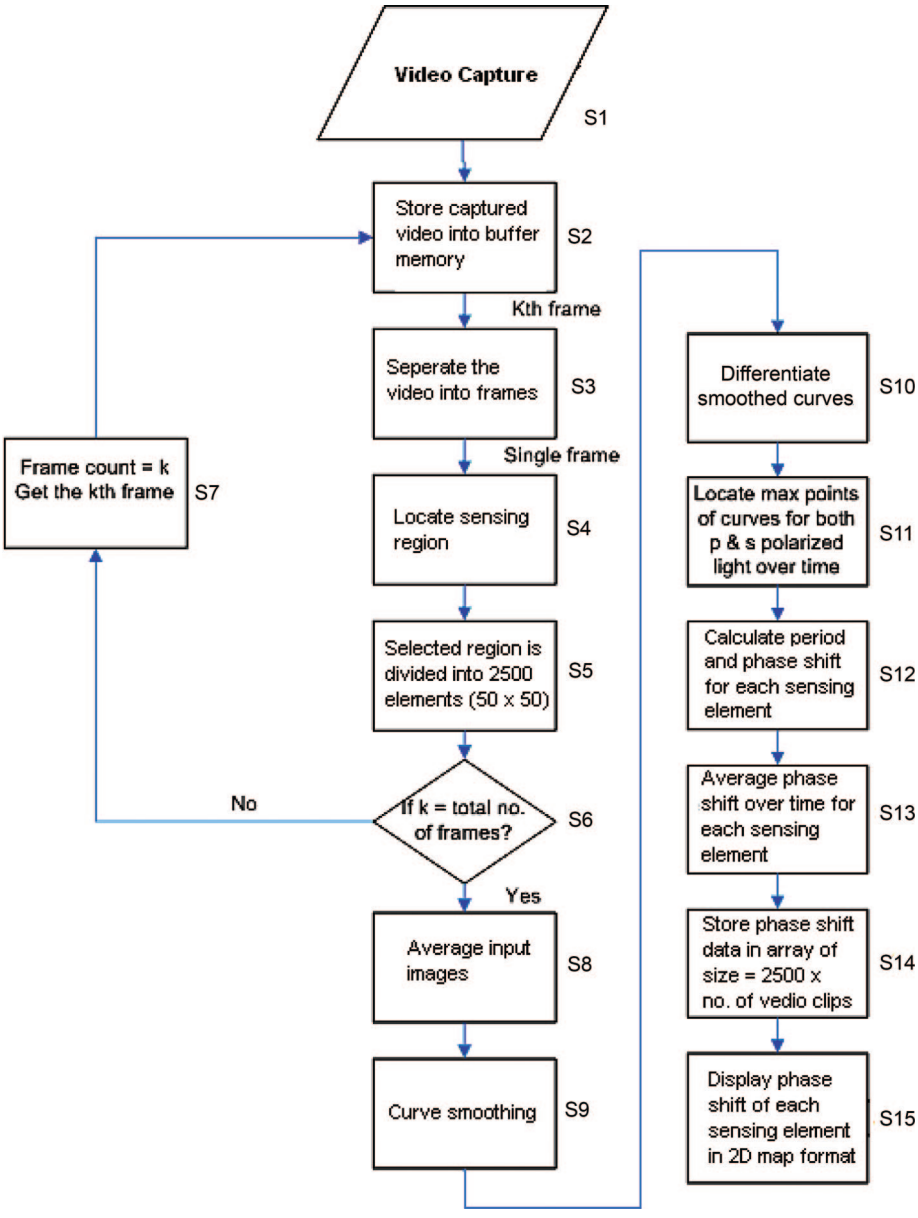

Fig. 2. (Color online) Flow chart of the phase extraction program.

used for the detections of bioaffinity interactions in DNA,[10–12] peptide,[13] protein,[14] and carbohydrate arrays.[15] Most of these research works are based on the SPR intensity imaging technique, which measures the reflectivity change caused by the refractive index change on the sensing surface. If an SPR image is taken at a fixed incident angle, the reflectance of any region within the sensor area is a function of the refractive index of the sample immediately next to the sensor surface.

As for phase-sensitive SPR sensing, this technique was first reported by Nelson.[16] Fresnel equations applied to the SPR situation predicts that the phase response has a steep slope over a small range of refractive index (RI) within the resonance peak. Phase-sensitive SPR may offer at least three times higher resolution than conventional angular SPR sensing approach. Until now, SPR imaging in the phase domain has been mainly focused on analyzing the fringe pattern of interferograms.[17–19] Spatial resolution over the sensor surface is limited and this makes it difficult to implement high-throughput microarray applications. Furthermore, phase detection is known to be extremely sensitive to environmental vibration.[18,19]

In this paper, we introduce a new approach, to the best of our knowledge, for performing phase-sensitive SPR imaging. A differential phase technique, which has been demonstrated in Ref. 20, is used to enhance the measurement stability of the system. The operation of this system is demonstrated by using salt-water mixtures. A microarray chip platform has also been adopted to demonstrate its potential capability for performing high-throughput protein detection.

2. Experiment

The configuration of the differential phase SPR imaging sensor is shown in Fig. 1. Laser beam from a 10 mW He–Ne laser is expanded by a 20× objective lens and a convex lens. The magnification of the beam is adjusted to cover a larger area of the sensing surface. In addition, an attenuator is incorporated for adjusting the beam intensity in order to avoid saturating the CCD imaging device (the quantization resolution of the CCD camera is 8 bit).

A Mach–Zehnder interferometer is used in the system for phase detection. A 50:50 beam splitter cube is used for separating the expanded laser beam into two paths. The first path I_S is for the probe arm and other path I_{Ref} is for the reference arm. In the probe arm, the beam enters a glass prism arranged in the Kretschmann configuration. The prism has an ~50 nm thick gold layer coated on the sensor surface[5] for exciting the required surface plasmon wave. The PDMS (polydimethylsiloxane) microchamber device is mounted on the sensor surface.[21] Each chamber is an independent cell. This ensures that a number of sensing measurements may be performed simultaneously. The size of each chamber is 1.5 mm in diameter and the distance between adjacent spots is 1.8 mm. The diameter of these microchambers can be further reduced too if necessary. In the reference arm, the laser beam is reflected by a plane mirror mounted on a piezoelectric transducer (PZT). With a saw-tooth wave drive signal at 0.1 Hz frequency, the PZT introduces a periodic linear phase shift to the reference optical beam.

When I_S and I_{Ref} recombine again at the second beam splitter, interference between them produces an interferogram. Since the two interfering beams are parallel to each other, intensity variations within the interferogram may provide the required SPR phase distribution caused by the sensing activity taking place at each sensor site. To achieve differential phase measurement, a Wollaston prism is placed in front of the CCD imaging device to separate the *p* and *s* polarizations. Since only *p* polarized light is affected by the SPR effect, information obtained from the *s* polarization serves as a reference signal. The optical system can be considered as two independent interferometers operating in parallel. Finally, interferometric phase stepping movies obtained from the *s* and *p* polarizations are captured by the CCD imaging device. The two interferometeric movies are then analyzed frame by frame using a computer, and the differential (i.e., SPR) phase distribution within the sensor surface is obtained.

3. Phase Extraction

During the experiment, the interference patterns were read in video format, and the intensity distribution for both *p* and *s* polarizations were analyzed using a home-built software written in MATLAB. A flow chart of the image analysis procedures is shown in Fig. 2.

The interference images are first read from the data source in video format (S1). Then, the selected sensor region within the image frame will be divided into 2500 elements (50 × 50) (S3) and the average intensity level for both *p* and *s* polarizations is extracted for each element. For each element, the av-

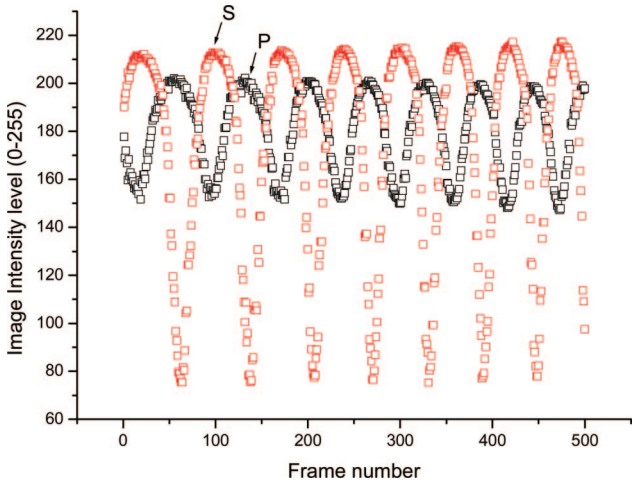

Fig. 3. (Color online) Typical interference intensity variations output from the image analyzing program, after feeding a series of image frames to the phase extraction program. Differential phase is obtained by analyzing the relative positions of the interference plots obtained from *p* and *s* polarizations.

erage intensity levels of all the frames within the video clip are stored in a separate data array (S8–S9). This data series, in fact, corresponds to an oscillating waveform due to the fact that the reference phase has been continuously swept while the imaging device is recording the interferograms. Figure 3 shows a typical intensity oscillation plot of an element for the *p* and *s* polarizations.

Fast Fourier transform (FFT) and low-pass filtering are used for reducing high-frequency noise (S9). After a differentiation operation (S10), the differential phase between *p* and *s* polarizations is obtained and comparing the peak positions of the two waveforms (S12). Finally, we obtain a two-dimensional (2D) phase map over the entire surface of the sensor region (S15) [as shown in Fig. 4(b)].

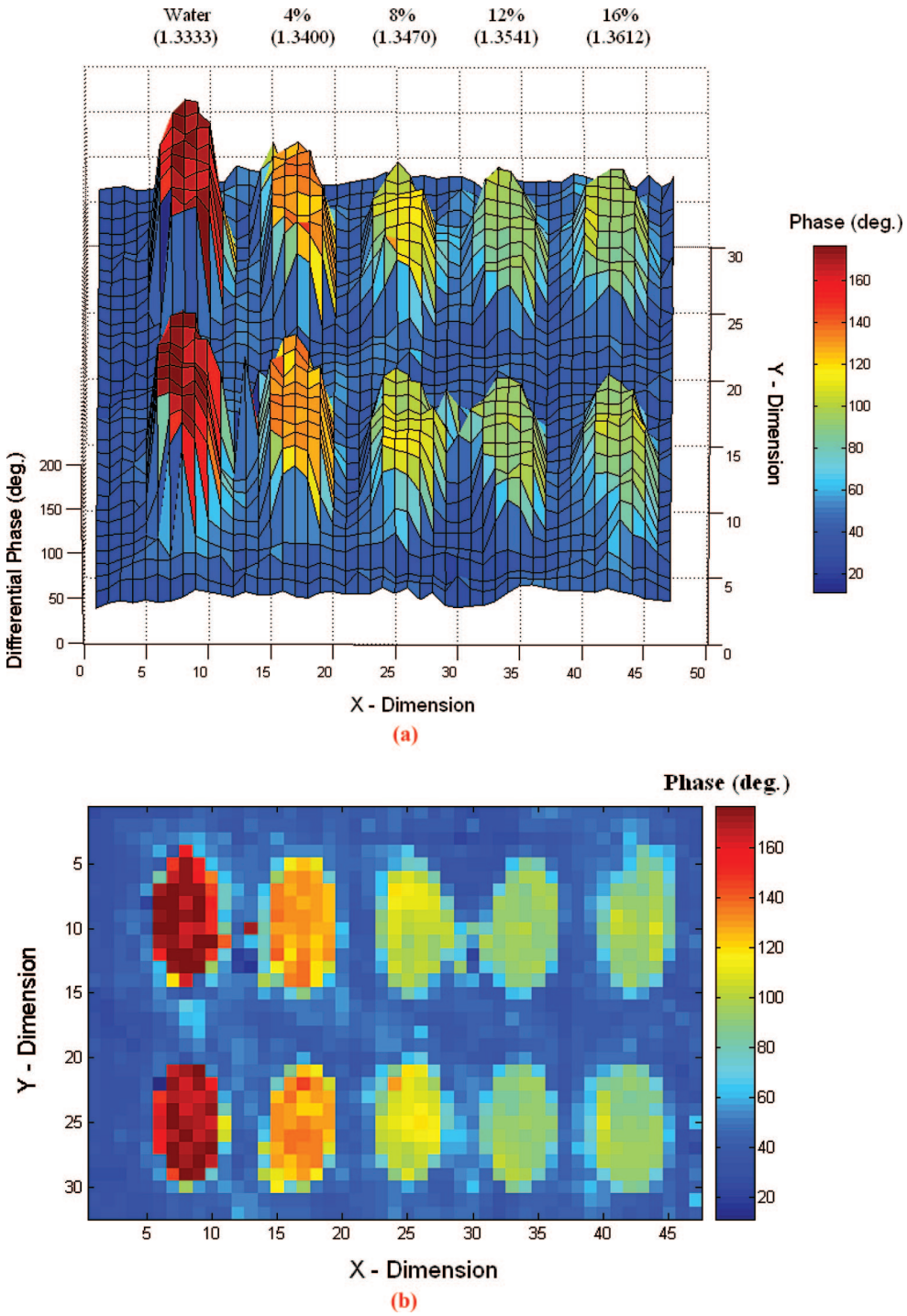

Fig. 4. Two-dimensional SPR phase map obtained from an array of salt solution sensor sites. Salt solution samples with concentrations ranging from 0% to 16% (1.3333–1.3612 RIU) are being measured simultaneously. Levels of phase responses are shown for different concentrations (174°–91°).

4. Results and Discussion

The operation of this system is demonstrated by using saltwater mixtures because of the ease of controlling the RI value of the analyte. In the experiment, we chose to use an array of salt solution sensing sites having salt concentrations ranging from 0% to 16% [in 4% steps, with a RI value of 1.3333–1.3612 RIU (Ref. 22)]. The PDMS microchambers were arranged in a 5 × 2 format. The salt solution samples were injected into the microchambers for SPR measurements.

During data capture, we took the averaged image data contents of 10 video clips, each 20 s long. The experimental differential SPR phase images are shown in Figs. 4(a) and 4(b). The SPR phase change, which is a function of the salt concentration, is shown as color variations. As the salt concentration increases from 0% to 16%, the color of the sensor spot changes from deep red to light green, which actually refers to a SPR phase change of ~174°.

Figure 5 shows a quantified version of the SPR phase change in relation to salt concentration. As indicated in Fig. 5(a), the average phase within a 7 pixels × 3 pixels area is extracted for each salt solution sensing site. The calculated average phase values for the sensor sites are plotted against the RI values of the salt solutions using information reported in Ref. 22. As shown in Fig. 5(b), response curves obtained from both rows of the samples are quite similar, thus confirming the reproducibility of this measurement technique.

We define that sensor sensitivity S refers to the sensor response Δx caused by a small refractive index change Δn given by the equation

$$S = \Delta n_s / \Delta x. \tag{1}$$

Sensor resolution R is the lowest detection limit that the SPR sensor can resolve. This parameter is affected by the measurement uncertainty standard deviation (SD), and the sensor sensitivity is described by the equation

$$R = S \cdot \mathrm{SD}. \tag{2}$$

A similar interpretation on sensor resolution has been reported by Nelson *et al.* in Ref. 16. In our experiment, $\Delta n_s/\Delta x$ refers to the slope of the response curve reported in Fig. 5(b). In the most sensitive region of the response curve (1.3333–1.3400 RIU), a change of 46.4° has been recorded for a 4% concentration increase (from water to 4% solution). SD in our case refers to the measurement standard deviation within ten measurements from the same sample. The experimental SD obtained from the reference sensor sites (in Row 1) with pure water as the analyte is 0.66°. Therefore, the corresponding SPR sensor resolution in terms of RI is 9.8×10^{-5} RIU.

In Fig. 5(b), we include the error bar (i.e., SD) obtained from different sensor sites corresponding to different salt concentrations. The error bars are used as an indicator on the refractive index measurement uncertainty for different sample solutions. The numerical SD values of different salt concentration samples are also listed in Table 1. The SD values are expected to improve through further adjustments in

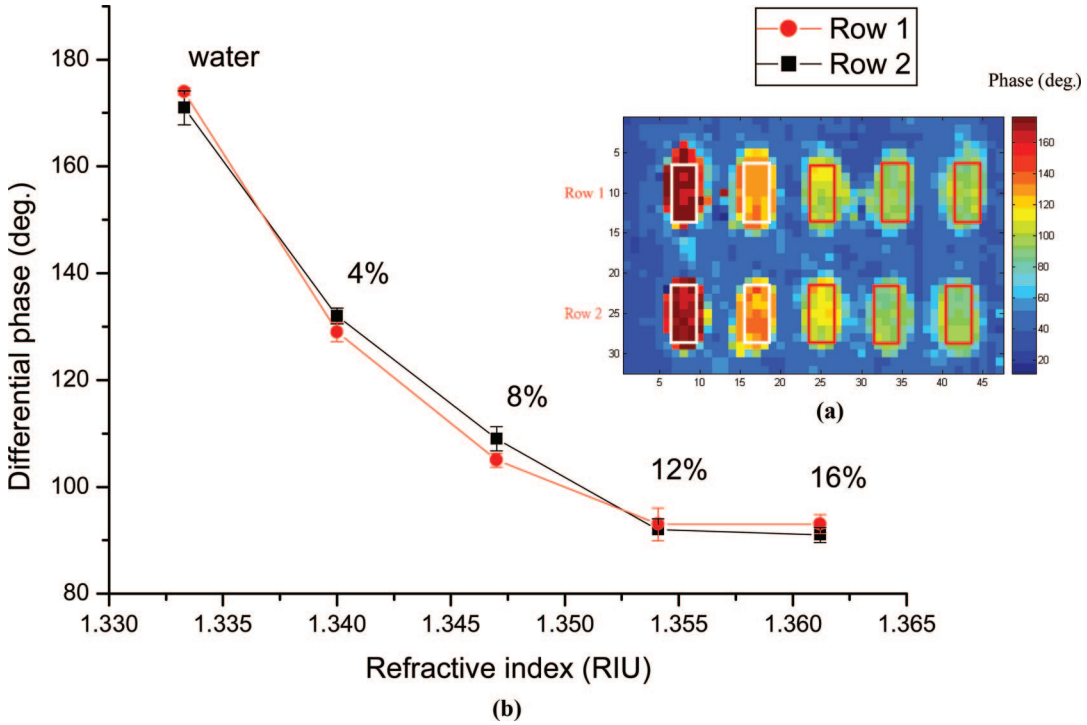

Fig. 5. Response curve of the phase SPR imaging sensor. (The phase values are extracted from a region containing in 7 pixels × 3 pixels in the phase map.)

Table 1. Measurement SD of Different Salt Concentration Samples

Salt Solution Concentration	Water	4%	8%	12%	16%
Refractive index (RIU)	1.3333	1.3400	1.3470	1.3541	1.3612
SD (Phase degree)	0.66	1.82	1.29	3.05	1.80

frame rate, interference pattern contrast, dynamic range of CCD camera, and involving a larger number of pixels during the image capturing process.

The sensor resolution is better than that reported by Xinglong *et al.*[19] Their data analysis technique is based on monitoring the relative position shift of interference fringes. The phase measurement accuracy depends critically on the number of fringes contained within each sensor site. High pixel count is therefore needed for each sensor site. This also poses severe limitation to the maximum achievable number of sensor sites per sensor array. On the other hand, the 2D SPR phase mapping approach reported in this paper alleviates this problem by moving the data capture from the spatial domain to the time domain. This means that, in principle, each pixel may act as an individual sensor site.

In the present technique, although one can use only one pixel per sensor site to achieve very high array density, in practice it might be better to have lower array density by having many pixels working for one sensor site. The mean phase value obtained from these pixels should contain less noise due to an averaging effect. In the actual experiment, we used pure water as the analyte. The SPR phase value of the sensing site was monitored for 45 min. Figure 6(a) shows one of the average phase maps, phase extraction was performed in different size of area (5 pixels $\times$ 5 pixels, 10 pixels $\times$ 10 pixels, etc.). The system uncertainty is plotted against the number of pixels used in phase extraction.

As revealed in Fig. 6(b), the standard deviation (SD) of the differential SPR phase measurement decreases with increasing number of pixels (N). This is in accordance with our intuitive expectation that SD decrease linearly with $\sqrt{N}$. This result therefore confirms that one can improve detection resolution simply by involving a larger number of pixels during the image capturing process. This means that if we use a high-resolution imaging device with very high pixel counts, which is what the current imaging device technology is pushing forward, we can immediately increase the measurement resolution without any penalty. Indeed, a similar argument is also valid, as far as increasing the performance of the system is concerned, when we increase the frame capture rate

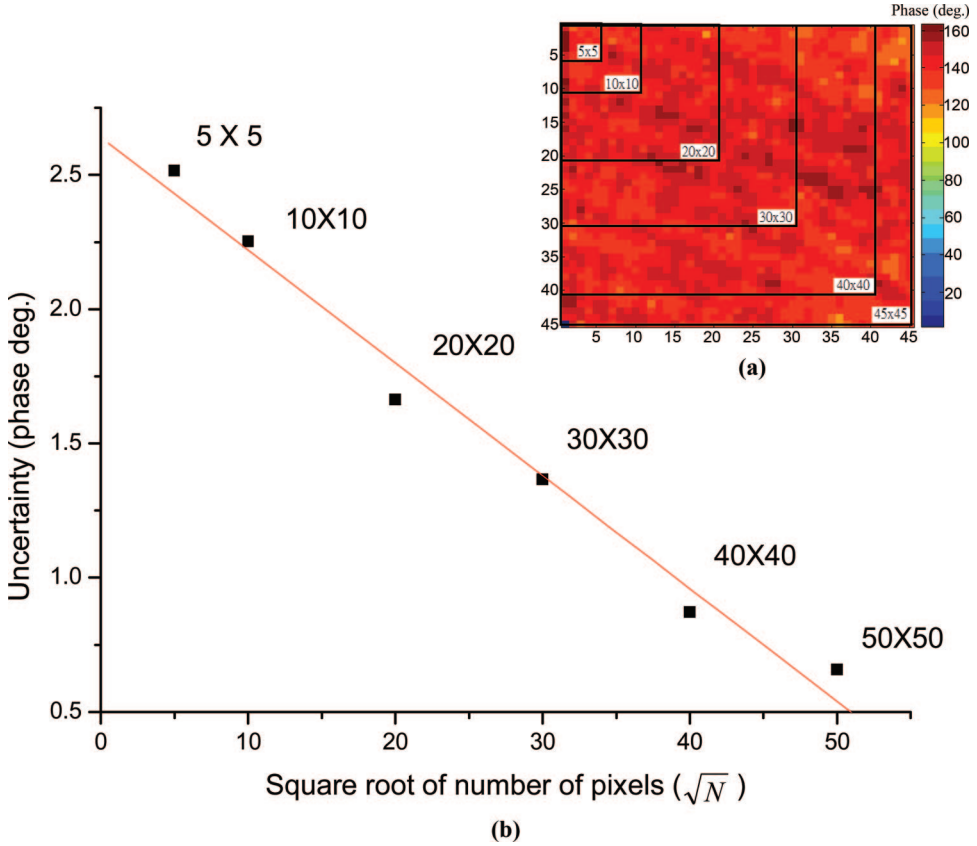

Fig. 6. (Color online) (a) Phase extraction was performed in different size of area (5 pixels $\times$ 5 pixels, 10 pixels $\times$ 10 pixels, etc.). (b) The system uncertainty is plotted against the number of pixels (N) used in phase extraction. The SD of the differential SPR phase measurement decreases linearly with increasing $\sqrt{N}$.

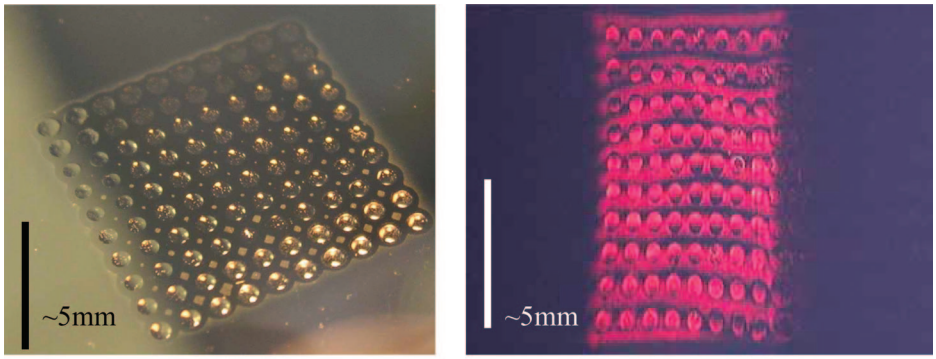

Fig. 7. (Color online) (a) Image of a microarray chip. It contains 100 elements within an area of 1 cm^2. (b) The microarray chip is integrated with a glass prism for SPR phase imaging measurement. The figure shows the corresponding SPR phase image.

(i.e., recording more data within a shorter time period). An experiment has been performed to study the behavior standard deviation (SD) in relation to the procedures of capturing the image frames. In the experiment, various modulation frequencies (2, 3, 4, and 5 Hz) were applied to the PZT modulator. At each frequency, ten videos were taken and the SD in 8% salt solution sensing was recorded. The measured SD was found to increase with decreasing number of captured image frames, i.e., the accuracy in phase extraction increases when we increase the number of frames analyzed. The SD is also closely related to the signal-to-noise ratio of the interference pattern. Improvement in the contrast of interference pattern enhances the accuracy in phase extraction. At resonance, the intensity of the incident beam is heavily attenuated by SPR absorption and this causes a relatively low fringe contrast in the resultant interference pattern. In our experiment, the reference beam in the Mach–Zehnder interferometer has been attenuated accordingly in order to improve the contrast of the interference pattern. In the experiment, the quantization resolution of the CCD camera is 8 bit. Since the dynamic range of the signal from the CCD chip affects the contrast of the interference pattern, the SD is expected to improve if one uses a CCD device with higher bit resolution.

5. Microarray Chip

Microarray chip is the current technology trend for high-throughput screening of bimolecular interactions. Indeed, the DNA microarray chip has already been widely used in gene expression and genotyping research.[2] With a 2D sensing capability, the present SPR phase imaging sensor might be able to provide parallel analysis of a large number of biomolecular interactions within a single experiment when it is integrate in microarray platform. Figure 7(a) shows a sample microarray chip containing 100 elements on an area of 1 cm^2. The size of each sensor spot is 400 μm in diameter and the distance between adjacent spots is 900 μm. When used in biosensing experiments, the microarray chip is attached to a glass prism using refractive index matching fluid. Two-dimensional SPR phase imaging is performed and each sensor region within the SPR phase image represents one sensor element. Figure 7(b) shows a typical SPR phase image of this 100 element microarray. Experiments are now on-going to populate the high-density microarrays with a variety of protein species and use the array for label-free diagnostic applications.

6. Conclusion

Biosensor arrays based on 2D detection of the SPR phase using a image capturing device has been demonstrated. The interferometric phase imaging system operates under a phase stepping mode and each pixel on the phase image may serve as an individual sensing element. The conventional SPR phase imaging approach is based on measuring the shift of fringe location in the interferogram, spatial resolution of the sensor device has been compromised, thus making it not possible for high density microarray designs. On the other hand, our phase measurement technique has alleviated this limitation by transforming the phase measurement mechanism from the spatial to time domain.

Our 2D SPR phase system has been shown to be capable of performing chemical sensing and detection of biomolecular interaction. The experimental sensor resolution is 9.8×10^{-5} RIU, which is comparable to the levels obtained from conventional phase imaging sensors based on fringe shift analysis.[18,19] Further improvement is possible if we change the imaging devices to a high performance version (i.e., high pixel count and large dynamic range). Given that there is a rapidly increasing need for better health monitoring technology because of the rising living conditions and an aging population, we anticipate that the label-free microarray biosensor device we report here should have a promising future and may find application in a variety of applications, including point-of-care diagnostics, protein chips, drug screening, etc.

The authors wish to acknowledge the funding support from the Research Grants Council, HKSAR, through a RGC Earmark Grant (project CUHK4186/04E) and The Shun Hing Institute of Advanced Engi-

neering, The Chinese University of Hong Kong. The authors thank L. T. Ho, Rebecca Chow, and Joyce Sze for their prayers.

References

1. D. Kambhampati, *Protein Microarray Technology* (Wiley-VCH, 2004).
2. N. Zammatteo, L. Jeanmart, S. Hamels, S. Courtois, P. Louette, L. Hevesi, and J. Remacle, "Comparison between different strategies of covalent attachment of DNA to glass surfaces to build DNA microarrays," Anal. Biochem. **280,** 143–150 (2000).
3. A. Ulman, "Formation and structure of self-assembled monolayers," Chem. Rev. **96,** 1533–1554 (1996).
4. K. L. Prime and G. M. Whitesides, "Self-assembled organic monolayers: model systems for studying adsorption of proteins at surfaces," Science **252,** 1164–1167 (1991).
5. J. Homola, S. S. Yee, and G. Gauglitz, "Surface plasmon resonance sensors: review," Sens. Actuators B **54,** 3–15 (1999).
6. J. Homola, "Present and future of surface plasmon resonance biosensors (review)," Anal. Bioanal. Chem. **377,** 528–539 (2003).
7. E. Yeatman and E. Ash, "Surface plasmon microscopy," Electron. Lett. **23,** 1091–1092 (1987).
8. B. Rothenhäusler and W. Knoll, "Surface-plasmon microscopy," Nature **332,** 615–617 (1988).
9. C. E. Jordan and R. M. Corn, "Surface plasmon resonance imaging measurements of electrostatic biopolymer adsorption onto chemically modified gold surfaces," Anal. Chem. **69,** 1449–1456 (1997).
10. E. A. Smith, M. G. Erickson, A. T. Ulijasz, B. Weisblum, and R. M. Corn, "Surface plasmon resonance imaging of transcription factor proteins: interactions of bacterial response regulators with DNA arrays on gold films," Langmuir **19,** 1486–1492 (2003).
11. E. A. Smith, M. Kyo, H. Kumasawa, K. Nakatani, I. Saito, and R. M. Corn, "Chemically induced hairpin formulation in DNA monolayers," J. Am. Chem. Soc. **124,** 6810–6811 (2002).
12. H. J. Lee, T. T. Goodrich, and R. M. Corn, "SPR imaging measurement of 1-D and 2-D DNA microarrays created from microfluidic channels on gold thin films," Anal. Chem. **73,** 5525–5531 (2001).
13. G. J. Wegner, H. J. Lee, and R. M. Corn, "Characterization and optimization of peptide arrays for the study of epitope-antibody interactions using surface plasmon resonance imaging," Anal. Chem. **74,** 5161–5168 (2002).
14. G. J. Wegner, H. J. Lee, G. Marriott, and R. M. Corn, "Fabrication of histidine-tagged fusion protein arrays for surface plasmon resonance imaging studies of protein-protein and protein-DNA interactions," Anal. Chem. **75,** 4740–4746 (2003).
15. E. A. Smith, W. D. Thomas, L. L. Kiessling, and R. M. Corn, "Surface plasmon resonance imaging studies of protein-carbohydrate interactions," J. Am. Chem. Soc. **125,** 6140–6148 (2003).
16. S. G. Nelson, K. S. Johnston, and S. S. Yee, "High sensitivity surface plasmon resonace sensor based on phase detection," Sens. Actuators B **35,** 187–191 (1996).
17. P. I. Nikitin, A. N. Grigorenko, A. A. Beloglazov, M. V. Valeiko, A. I. Savchuk, O. A. Savchuk, G. Steiner, C. Kuhne, A. Huebner, and R. Salzer, "Surface plasmon resonance interferometry for micro-array biosensing," Sens. Actuators A **85,** 189–193 (2000).
18. H. P. Ho and W. W. Lam, "Application of differential phase measurement technique to surface plasmon resonance sensors," Sens. Actuators B **96,** 554–559 (2003).
19. Y. Xinglong, W. Dingxin, W. Xing, D. Xiang, L. Wei, and Z. Xinsheng, "A surface plasmon resonance imaging interferometry for protein micro-array detection," Sens. Actuators B **108,** 765–771 (2005).
20. S. Y. Wu, H. P. Ho, W. C. Law, C. Lin, and S. K. Kong, "Highly sensitive differential phase-sensitive surface plasmon resonance (SPR) biosensor based on Mach–Zehnder configuration," Opt. Lett. **29,** 2378–2381 (2004).
21. B.-H Jo, L. M. Van Lerberghe, K. M. Motsegood, and D. J. Beebe, "Three-dimensional micro-channel fabrication in polydimethylsiloxane (PDMS) elastomer," J. Microelectromech. Syst. **9,** 76–81 (2000).
22. R. C. Weast, ed. *CRC Handbook of Chemistry and Physics,* 68th ed. (CRC, 1987).